

# Low Energy Properties of Ferrimagnetic 2-leg Ladders: a Lanczos study

A. Langari<sup>†</sup> and M.A. Martín-Delgado<sup>\*</sup>,

<sup>†</sup> *Max-Planck-Institut für Physik komplexer Systeme, Nöthnitzer Strasse 38, D-01187 Dresden, Germany*

<sup>\*</sup> *Departamento de Física Teórica I, Universidad Complutense, 28040-Madrid, Spain.*

We apply the Lanczos method to a 2-leg ladder with mixed spins of magnitudes  $(S_1, S_2) = (1, 1/2)$  located at alternating positions along the ladder. The effect of dimerization  $\gamma$  is also considered according to two different patterns. A Spin Wave Theory (SWT) is applied to this model predicting one gapless branch with ferromagnetic properties and another gapped branch with antiferromagnetic nature as low energy excitations of the model. We compute the ground state energies, Ferro- and AF-excitation gaps, magnetizations and correlation functions as a function of  $J'$  and  $\gamma$  which results into a fine estimate of the phase diagram. The Lanczos results are compared with the SWT analysis and a qualitative agreement is found but with numerical discrepancies. We also study numerically the Spin-Peierls instability and find that it is conditional for any value of  $J' \in (0, 2)$  and both dimerization patterns.

PACS number: 76.50.+g, 75.50.Gg, 75.10.Jm

## I. INTRODUCTION

Mixed spin chains with alternating spins  $(1, 1/2)$  are paradigmatic examples of strongly correlated systems exhibiting excitations of different types, namely, both gapless and gapped excitations in the low energy spectrum [1–4]. This is a manifestation of their ferrimagnetic character and they are responsible for their unusual properties. On the contrary, one-dimensional integer-spin Anti-ferromagnetic Heisenberg (AFH) model has a unique disordered ground state with a finite excitation gap while the half-integer spin AFH chain is gapless [5]. These ferrimagnetic quantum chains have recently attracted much attention and several techniques have been devoted to their study: analytically, such as Spin Wave Theory (SWT) [2,3], Quantum Renormalization Group [6], Variational [1], and numerically, such as conventional [3], transfer matrix DMRG [4], QMC [4] etc... Moreover, the interest is increased due to the fact that experimental realizations of these one-dimensional ferrimagnets also exist. For instance, the oxamate compound  $NiCu(pba)(D_2O)_3 \cdot 2D_2O$  exhibits a structure of a  $(S_1, S_2) = (1, 1/2)$  ferrimagnetic chain [7] where the spins 1 are located at the Ni sites and the spins  $1/2$  at the Cu sites. It is found that below  $T = 7K$  it exhibits Long Range Order (LRO). Materials realizing other magnitudes of spins  $(S_1, S_2)$  have been also synthesized [8]. In all these compounds it is assumed that the interchain coupling is much smaller than the intra-chain interactions so that the system becomes a set of effectively uncoupled quantum chains.

On the other hand, many interesting investigations have been devoted to spin ladders. They consist of coupled one-dimensional chains and may be regarded as interpolating one- and two-dimensional systems. Theoretical studies have suggested two different universal-

ity class for the uniform spin ladders, i.e. the antiferromagnetic spin- $\frac{1}{2}$  ladders are gapped or gapless, depending on whether  $n_l$  (the number of legs) is even or odd [9]. Some experimental observations are in agreement with this results [10]. However mixed-spin ladders may change this universality. In a recent work [11] we have considered a ferrimagnetic 2-leg ladder and conjectured its phase diagram by using an approximate Quantum RG analysis. We have shown that for the homogeneous antiferromagnetic couplings the model is gapless but an energy gap may appear in a specific type of configuration of the coupling constants.

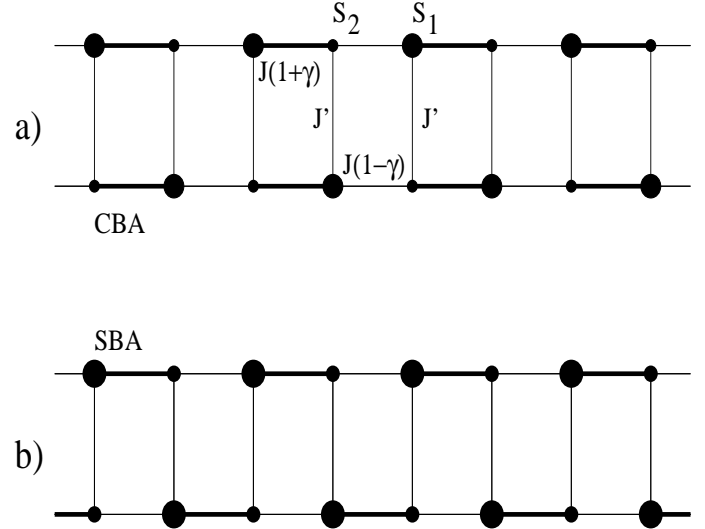


FIG. 1. A picture of the dimerization patterns considered in a 2-leg mixed spin ladder: a) Columnar Bond Alternation (CBA), b) Staggered Bond Alternation (SBA). Small circles are  $S = \frac{1}{2}$  and large ones are  $S = 1$ .

In this work we present the results of an extensive numerical analysis using the Lanczos method [10] applied

to a large class of ferrimagnetic 2-leg ladders for the first time (see [9] for a review on ladder materials.) Apart from accurate numerical results which show the effect of inter-chain interaction in a ferrimagnetic system, we obtain the phase diagram of Ref. [11] with more accuracy. In the present phase diagram, which is obtained by Lanczos results, we specify the phase boundary between the gapless and gapped phases more accurately and show that the transition between two gapless phases appears at zero inter-chain coupling and is first-order. An analytic Spin Wave Theory is also introduced to describe the low-energy excitations of this model. Moreover we will consider the effect of bond-alternation on the Spin-Peierls instability and its conditional or unconditional character. The model we have considered here, depicted in Fig.1, can be assumed as the first step to consider the inter-chain interactions in a ferrimagnetic material. (For instance,  $MnCu(pbaOH)(H_2O)_3$  has such kind of structure [12].) In our model mixed spins have lengths  $S_1 = 1$  and  $S_2 = 1/2$  and are located at alternating positions in this bipartite lattice, making up the sub-lattices A and B, respectively. One may think of two  $(1, 1/2)$  ferrimagnetic chains which interact via rungs in a ladder realization where different kind of spins are located on each rung (see Fig.1). Specifically, the isotropic Heisenberg Hamiltonian we consider is the following ( with  $i = 2n + \alpha$ ),

$$\begin{aligned}
H = & J \sum_{\alpha=1}^2 \sum_{n=0}^{\frac{L}{2}-1} ( [1 + \gamma^{(\alpha)}(i)] \mathbf{S}_1^{(\alpha)}(i) \cdot \mathbf{S}_2^{(\alpha)}(i+1) \\
& + [1 + \gamma^{(\alpha)}(i+1)] \mathbf{S}_2^{(\alpha)}(i+1) \cdot \mathbf{S}_1^{(\alpha)}(i+2) ) \\
& + J' \sum_{n=0}^{\frac{L}{2}-1} [\mathbf{S}_1^{(1)}(2n+1) \cdot \mathbf{S}_2^{(2)}(2n+1) \\
& + \mathbf{S}_2^{(1)}(2n+2) \cdot \mathbf{S}_1^{(2)}(2n+2)] , \quad (1)
\end{aligned}$$

where  $\mathbf{S}_1^{(\alpha)}(n)$  denotes the quantum spin-1 at site  $n$  in the leg  $\alpha = 1, 2$  of the ladder, similarly  $\mathbf{S}_2^{(\alpha)}(n)$  for the spin-1/2,  $J$  and  $J'$  are coupling constants along the legs and the rungs respectively, and  $\gamma^{(\alpha)}(n)$  is the dimerization patterns. We consider two different dimerization patterns : i) CBA (Columnar Bond Alternation, Fig.1(a)) for which  $\gamma^{(\alpha)}(n) = (-1)^{n+1}\gamma$  [11], and ii) SBA (Staggered Bond Alternation, Fig.1(b)) where  $\gamma^{(\alpha)}(n) = (-1)^{\alpha+1+n}\gamma$  [13,14]. In order to keep the system always in the antiferromagnetic regime, we restrict the range of variation as  $|\gamma| \leq 1$ . We use periodic boundary conditions along the legs of the ladder. The number of sites is  $N = 2 \times L$ , where  $L$  is the length.

The paper is organized as follows: in next section we introduce the spin wave theory applied to a non-dimerised ( $\gamma = 0$ ) ferrimagnetic  $(S_1, S_2)$  ladder. Dispersion relations, ground state energy, energy gap and magnetization of this model are obtained within SWT in order to explain the nature of elementary excitations in

this system. In Sec. III we present our numerical results obtained with the Lanczos method and we contrast them against the previous SWT results. In Sec. IV we extend our Lanczos results to include a numerical analysis of the phase diagram for a 2-leg mixed spin ladder to specify the boundary between the gapless and gapped phases. In Sec. V. the spin-Peierls instability is discussed by computing the magnetic energy gain of the present model. We finally present our conclusions in Sec. VI.

## II. SPIN WAVE THEORY

In this section we shall perform a mean-field treatment of the ferrimagnetic ladders and for simplicity we shall concentrate on the case of zero dimerization  $\gamma = 0$ .

The application of the Lieb-Mattis theorem [15] to this ferrimagnetic ladder predicts the existence of a Ground State (GS) with Total Spin  $S_G$  given by  $S_G = L(S_1 - S_2)$ . This leads to the existence of a non-vanishing value of the magnetization at zero temperature. Then, a natural issue arises, namely, the study of classical ferrimagnetic order v.s. quantum antiferromagnetic fluctuations [6]. This system presents gapless Ferromagnetic excitations (Goldstone modes due to broken symmetry) with spin  $S_G - 1$  and gapped Antiferromagnetic excitations with spin  $S_G + 1$ .

Thus, as we expect an ordered ground state, it is natural to perform a spin wave theory analysis to describe the low energy quantum fluctuations around a classical ferrimagnetic ground state. We shall employ the SWT in the linear approximation.

To this end, we first make a standard Holstein-Primakoff transformation on the  $(1, 1/2)$ -spins of eq. (1). Let  $a_k^{(\alpha)}$  be the modes in momentum space associated to the sub-lattice A for the legs  $\alpha = 1, 2$ , and  $b_k^{(\alpha)}$  similarly for the modes in the sub-lattice B. The Hamiltonian can be written in the following form.

$$H_{SWT} = H_{rung} + \sum_{\alpha=1,2} H_{leg}^{(\alpha)}$$

$$\begin{aligned}
H_{rung} = & -LJ'S_1S_2 \\
& + J' \sum_k [S_1(a_k^{\dagger(1)}a_k^{(1)} + a_k^{\dagger(2)}a_k^{(2)}) + S_2(b_k^{\dagger(1)}b_k^{(1)} + b_k^{\dagger(2)}b_k^{(2)})] \\
& + J'\sqrt{S_1S_2} \sum_k (a_k^{(1)}b_k^{(2)} + a_k^{(2)}b_k^{(1)} + a_k^{\dagger(1)}b_k^{\dagger(2)} + a_k^{\dagger(2)}b_k^{\dagger(1)})
\end{aligned}$$

$$\begin{aligned}
H_{leg}^{(\alpha)} = & -LJS_1S_2 + 2J \sum_k (S_1 a_k^{\dagger(\alpha)} a_k^{(\alpha)} + S_1 b_k^{\dagger(\alpha)} b_k^{(\alpha)}) \\
& + J\sqrt{S_1S_2} \sum_k 2\text{Cos}(k)(a_k^{(\alpha)} b_k^{(\alpha)} + a_k^{\dagger(\alpha)} b_k^{\dagger(\alpha)}) \quad (2)
\end{aligned}$$

As it is apparent, this is not enough to diagonalize the Hamiltonian with a Bogoliubov transformation because

the degrees of freedom of each leg appear coupled together. Fortunately enough, we can devise a second transformation by introducing a couple of symmetric  $s', s''$  and antisymmetric  $a', a''$  fields as follows:

$$\begin{aligned} a^{(\alpha)} &= \frac{1}{\sqrt{2}}(s'_k + (-1)^{1+\alpha} a'_k), \\ b^{(\alpha)} &= \frac{1}{\sqrt{2}}(s''_k + (-1)^{1+\alpha} a''_k), \end{aligned} \quad (3)$$

with  $\alpha = 1, 2$  represents leg index. Then, it is possible to show that the resulting SWT Hamiltonian takes the following form in terms of these fields:

$$H_{SWT} = -LS_1S_2(2J + J') + h(s) + h(a), \quad (4)$$

where

$$\begin{aligned} h(s) &= C_1 \sum_k s'_k{}^\dagger s'_k + C_2 \sum_k s''_k{}^\dagger s''_k \\ &+ \sqrt{S_1S_2} \sum_k (J2 \cos k + J')(s'_k s''_k + s'_k{}^\dagger s''_k{}^\dagger), \end{aligned} \quad (5)$$

$$\begin{aligned} h(a) &= C_1 \sum_k a'_k{}^\dagger a'_k + C_2 \sum_k a''_k{}^\dagger a''_k \\ &+ \sqrt{S_1S_2} \sum_k (J2 \cos k - J')(a'_k a''_k + a'_k{}^\dagger a''_k{}^\dagger), \end{aligned} \quad (6)$$

and now using a set of Bogoliubov transformations we will arrive at the following expressions for these Hamiltonians  $h(s)$ ,  $h(a)$  as,

$$\begin{aligned} h(s) &= \sum_k [\zeta^{(+)}(k) + \omega_A^{(+)}(k) A_k^{(+)} A_k^{(+)} + (A_k^{(+)} \leftrightarrow B_k^{(+)})], \\ h(a) &= \sum_k [\zeta^{(-)}(k) + \omega_B^{(-)}(k) B_k^{(-)} B_k^{(-)} + (B_k^{(-)} \leftrightarrow A_k^{(-)})], \end{aligned} \quad (7)$$

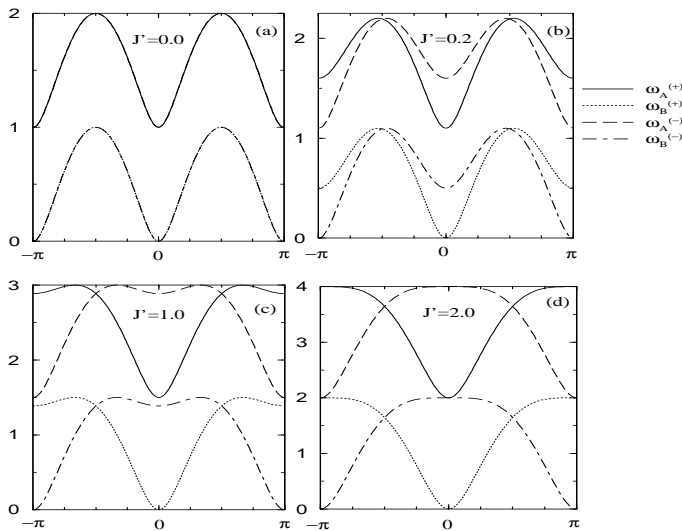


FIG. 2. Dispersion relations for a ferrimagnetic ladder for different values of rung coupling namely  $J' = 0.0, 0.2, 1.0, 2.0$ . The  $J' = 0$  case (a) is the same as one-dimensional ferrimagnets.

where  $A_k^{\dagger(\pm)}, B_k^{\dagger(\pm)}$  are the quasi-particle creation operators and the frequencies  $\omega_A^{(\pm)}(k), \omega_B^{(\pm)}(k)$  of the several excitations take the following expressions as a function of the model coupling constants,

$$\begin{aligned} \omega_A^{(\pm)}(k) &= \frac{1}{2}(C_1 - C_2 + \sqrt{(C_1 + C_2)^2 - 4C_3^{2(\pm)}(k)}), \\ \omega_B^{(\pm)}(k) &= \frac{1}{2}(C_2 - C_1 + \sqrt{(C_1 + C_2)^2 - 4C_3^{2(\pm)}(k)}), \\ \zeta^{(\pm)}(k) &= -\frac{1}{2}(C_1 - C_2) + \frac{1}{2}\sqrt{(C_1 + C_2)^2 - 4C_3^{2(\pm)}(k)}, \\ C_1 &= (2J + J')S_1 \quad C_2 = (2J + J')S_2, \\ C_3^{(\pm)}(k) &= \sqrt{S_1S_2}(2J \cos k \pm J'), \end{aligned} \quad (8)$$

In Fig.2 we have plotted the four branches of the dispersion relations  $\omega_A^{(\pm)}(k), \omega_B^{(\pm)}(k)$ . For vanishing inter-chain coupling  $J' = 0$  (Fig. 2 (a)) we reproduce the 1d-chain result. As the interaction is switched on, we appreciate the splitting of each zero-coupling branch into another two new branches in the case of ladder. The appearance of four modes is related to defining two boson operators for each leg of ladder. At  $k = 0$  we define the gap as  $g_1 \equiv |\omega_B^{(+)}(0) - \omega_B^{(-)}(0)|$ , which goes to zero with vanishing  $J'$  as can be seen in Fig.3. We also define the gap  $g_2 \equiv |\omega_A^{(+)}(0) - \omega_B^{(+)}(0)|$ , which remains finite  $\forall J'$  (see Fig.3). So we consider  $g_2$  as the actual energy gap which is defined by SWT. The lowest energy dispersion relation is  $\omega_B^{(+)}$  which shows gapless excitations at  $k = 0$ ,

$$\omega_B^{(+)}(k \rightarrow 0) = \frac{2S_1S_2J}{|S_1 - S_2|} k^2 \quad (9)$$

The first excited branch which shows an actual gap for any value of  $J'$  is  $\omega_A^{(+)}$  with the following behaviour in the long wave length limit,

$$\omega_A^{(+)}(k \rightarrow 0) = (2J + J')|S_1 - S_2| + \frac{2S_1S_2J}{|S_1 - S_2|} k^2 \quad (10)$$

Eq.(9) is similar to a ferromagnetic dispersion relation, then we expect a ferromagnetic behaviour for these excitations. Moreover it can be shown that the  $\omega_B^{(+)}(k)$  modes are created by acting on the classical ferrimagnetic ordered state ( $|0\rangle$ ) with  $S_k^- = \frac{1}{\sqrt{L}} \sum_n \sum_\alpha (S_1^{-(\alpha)}(n) + S_2^{-(\alpha)}(n)) e^{ikn}$ , where  $k \neq 0$ . The outcomes of this operation are those states which have  $S_{tot}^z = L|S_1 - S_2| - 1$ . These states are annihilated by  $S_{tot}^+$ . Therefore we conclude that these states have  $S_{tot} = L|S_1 - S_2| - 1$  which is another sign for the ferromagnetic behaviour of  $\omega_B^{(+)}$  modes. The magnetization of  $S_1 = 1$  sub-lattice shown in Fig.(4) verifies the reduction of magnetization from its classical value ( $\langle S_1^z \rangle_{class.} = 1$ ) which shows that the quantum fluctuations of the lowest branch has a ferromagnetic property. Similarly, the  $\omega_A^{(+)}$  modes are created by acting on  $|0\rangle$  with  $S_k^+ = \frac{1}{\sqrt{L}} \sum_n \sum_\alpha (S_1^{+(\alpha)}(n) +$

$S_2^{+(\alpha)}(n)e^{ikn}$ , where  $k \neq 0$ . It is also possible to show that those states have  $S_{tot} = L|S_1 - S_2| + 1$  which is the property of an anti-ferromagnetic excitations, i.e. the excited states have larger spin than the ground state. All of these explanations for the excited states are examined for a finite system size ( $N = 2L = 8, 12, 16, 20$ ) by Lanczos method where we will discuss them in the next section.

Using the quantities  $\zeta^{(\pm)}(k)$  and eqs. (3)-(8), we have also computed the GS energy per site  $E_0/JN$  as follows,

$$E_0 = -NS_1S_2(2J + J') + \sum_k (\zeta^{(+)}(k) + \zeta^{(-)}(k)). \quad (11)$$

It is plotted as a function of  $J'$  in Fig.3.

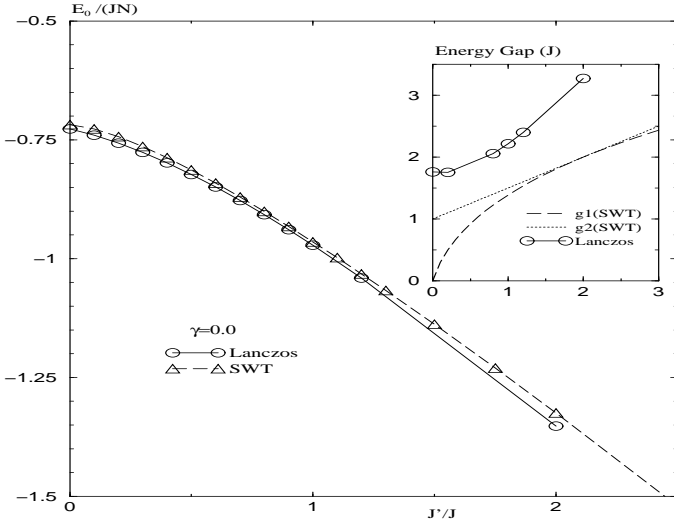


FIG. 3. Lanczos v.s. SWT results for GS energy, as a function of the interchain coupling  $J'$ . Inset similarly shows the Lanczos results v.s. SWT for energy gaps.

In a similar way the sub-lattice magnetization  $m_1$  as a function of the couplings is calculated,

$$m_1 = \frac{1}{L} \sum_{i=1}^{L/2} \langle S_1^{z(1)}(i) + S_1^{z(2)}(i) \rangle. \quad (12)$$

The other sub-lattice magnetization  $m_2 = \langle S_2^z \rangle$  can also be obtained by using the identity :  $m_1 + m_2 = S_1 - S_2$ . We have plotted  $m_1$  as a function of  $J'$  in Fig.4. We will discuss on this result in the next section.

### III. NUMERICAL ANALYSIS: LANCZOS METHOD

Let us now present our numerical Lanczos results. We have studied ladders with a number of sites  $N = 2 \times L$  with  $L = 4, 6, 8, 10$  due to the constraint of periodic BC's. We always set  $J = 1$  and vary  $J' = 0.0, 0.2, 0.8, 1.0, 1.2, 1.8, 2.0$ . The dimerization parameter

is varied from  $\gamma = 0.0$  to  $\gamma = 1.0$  in steps of 0.2 for both CBA and SBA patterns.

As a testground, we have checked several quantities at  $J' = 0$ , like the GS energy per site  $e_0$  and Antiferromagnetic gap  $\Delta_0$  and we find excellent agreement with the DMRG results for the spin chain as shown in Table 1, namely,  $e_0(DMRG) = -0.727$  and  $\Delta_0(DMRG) = 1.759$  [3,4].

In Fig. 3 we plot the variation with  $J'$  of the GS energy and we find that the extrapolated numerical results agree very well with the SWT results in the whole range. However, for the Antiferromagnetic gap (see inset of Fig.3) we find clear numerical differences with SWT. For comparison, we have plotted the two gaps,  $g_1, g_2$  introduced before, because for the strong coupling region around  $J' \sim 2$ , both gaps turn out to be very close to each other. We clearly find that the exact gap obtained with Lanczos is well above the values obtained with the SWT approximation.

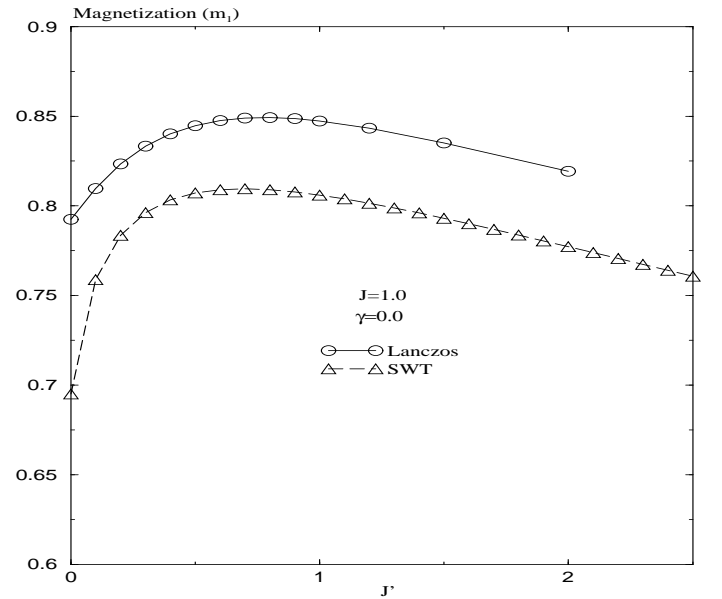


FIG. 4. Sub-lattice magnetization of spin  $S_1 = 1$  ( $\langle S_1^z \rangle$ ), Lanczos v.s. SWT results as a function of  $J'$ .

Likewise, we have computed several sub-lattice magnetization and in Fig. 4 we show  $m_1 = \langle S_1^z(1) \rangle$  for the spin-1 case at site  $n = 1$  and we have checked that it is the same at all other positions due to translational invariance. We find that the SWT calculation essentially underestimates the Lanczos result. The discrepancies between SWT results for energy gap (inset of Fig. 3) and magnetization (Fig. 4) means that the linear SWT does not provide us with a complete account of quantum fluctuations around the classical ferrimagnetic order. However the ground state energy obtained by both methods are in good agreement. For instance in the homogeneous case ( $\gamma = 0, J = 1, J' = 1$ ) the SWT result is  $e_0(SWT) = \frac{E_0}{JN} = -0.96475$  which has only 0.7 percent error with respect to Lanczos result (Table.1).

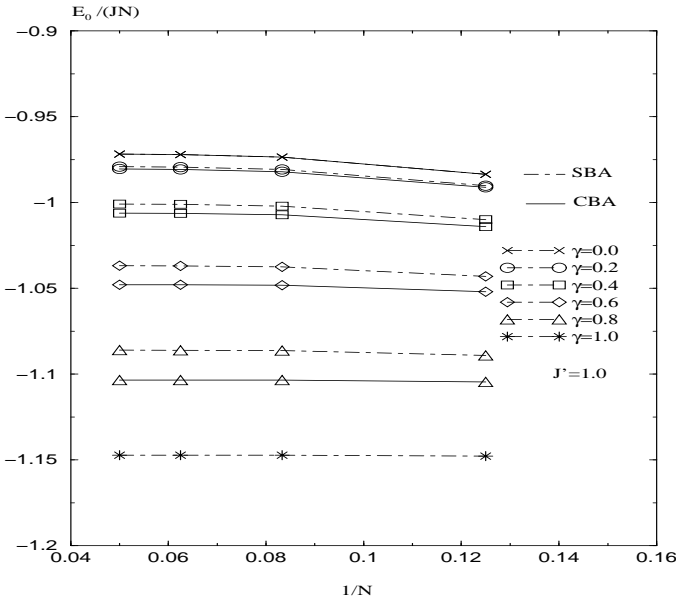


FIG. 5. Plot of the GS energy (Lanczos) v.s.  $1/N$  for CBA and SBA dimerization patterns. Convergence to thermodynamic limit is very sharp for all dimerization value ( $\gamma$ ).

We have also studied the effect of dimerization in the ferrimagnetic 2-leg ladder in the Columnar (CBA) and staggered (SBA) configurations. In Fig.5 we present the results of Lanczos calculations for  $J' = 1$  and varying the staggering parameter  $\gamma$  in the whole range. We first check that our results are well converged for the sizes considered ( $N=8,12,16,20$ ). The ground state energy converges to the value of thermodynamic limit as rapid as in the one-dimensional ferrimagnets. It means that the finite size effects are small in the ferrimagnetic ladders as well as in 1-D models. We then observe that the effect of dimerization ( $\gamma$ ) is generically to decrease the GS energy and that the columnar configuration produces a bigger energy decrease than the staggered pattern. This shows that the CBA pattern is more stable than the SBA configuration. The stability is improved by increasing dimerization.

$J'$	0.0	0.1	0.2	0.3	0.4	0.5
$e_0$	-0.7270	-0.7403	-0.7569	-0.7764	-0.7985	-0.8229
$J'$	0.6	0.7	0.8	1.0	1.2	2.0
$e_0$	-0.8493	-0.8776	-0.9075	-0.9716	-1.0408	-1.3524
$J'$	0.0	0.2	0.8	1.0	1.2	2.0
$\Delta_0$	1.7589	1.7544	2.0545	2.2158	2.3981	3.2696

Table 1. Extrapolated ( $N \rightarrow \infty$ ) Lanczos results for GS density energy  $e_0 = E_0/JN$  and AF-gap  $\Delta_0$ .

The Lanczos analysis of the ferromagnetic and anti-ferromagnetic gaps are shown in Figs.6. In Fig.6(a) we clearly find that in the absence of dimerization  $\gamma = 0$ , the Ferro-gap  $E_0(S_G - 1) - E_0(S_G)$  scales to zero as the system size  $N$  goes to  $\infty$ . This corresponds to the gapless excitations in the SWT analysis. We have plotted data

for different values of  $J'$  (0.8, 1.0, 1.2, 2.0) which shows the same behaviour. We have also checked for some more values of  $J'$  and the same results are obtained. Moreover, we have found that this also holds true when dimerization is present and in Fig.6(c) we show this for the SBA configuration which shows that we have gapless excitations with ferromagnetic nature for all values of  $J'$  and the dimerization parameters ( $\gamma$ ). In Figs.6(b),(d) we have plotted the AF-gap  $E_0(S_G + 1) - E_0(S_G)$  for some values of  $J'$  and  $\gamma$ . We find that the AF-gap remains finite in the thermodynamic limit, moreover the interchain coupling  $J'$  increases the gap both with or without dimerization. The notion of Ferro-gap and AF-gap is related to the excitations with spin lower or higher than the spin of the ground state, respectively. This is in complete agreement with the SWT explanation of the low energy spectrum.

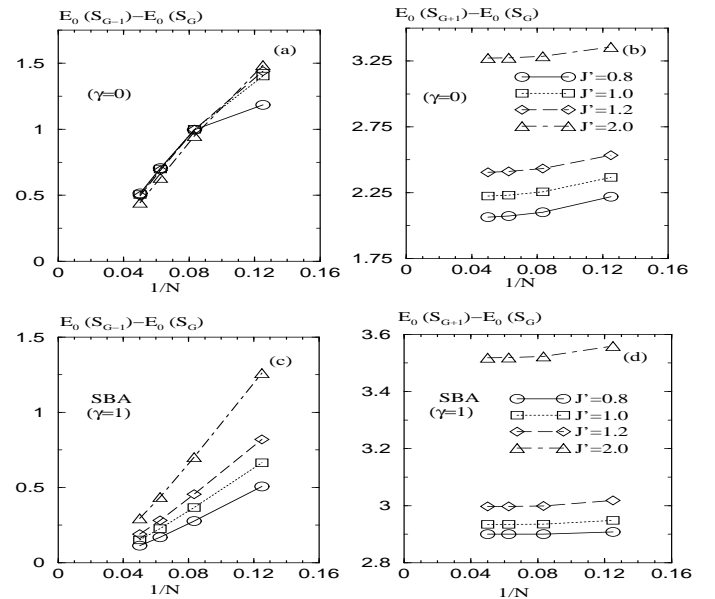


FIG. 6. Plot of energy gaps (Lanczos): (a)-(b) Ferro-gap and AF-gap without dimerization v.s.  $1/N$  for several couplings  $J'$ . (c)-(d) Same with dimerization (SBA).

We have presented the extrapolated values of ground state energy per site ( $e_0$ ) and AF-gap ( $\Delta_0$ ) in Table 1. The scaling form which we have considered for the extrapolation to  $N \rightarrow \infty$  is a power-law fit. We have implemented the following function for the scaling form of the ground state energy,

$$e_0(N) = e_0(\infty) + \frac{a}{N^\nu} \quad (13)$$

where  $a$  and  $\nu$  are constants and obtained to have least-square root error. We have examined a polynomial form but the best fitting was obtained by the power-law fit of Eq.(13). In the case of energy gap we considered both Eq.(13) and an exponential form, (i.e.  $\Delta_0(N) = \Delta_0(\infty) + B \exp(-|c|N)/(N^\mu)$ ) where  $B$ ,  $c$  and  $\mu$  are constants. Both scaling forms give us the same results for

$\Delta_0(\infty)$  and fit very well to the data of Fig.(6). Although from the SWT calculations we obtained the  $k^2$  dependence for both gapless and gapped spectrum (Eqs.(9, 10)) which impose that the scaling form should be like  $N^{-2}$ , however this type of function does not fit to our data and leads to a big value for the square least error.

In Figs.7 we present our numerical analysis of the two-point GS correlation functions (Eq.(14)) for spin-1-spin-1 ( $\sigma, \sigma' = (1, 1)$ ) and spin-1/2-spin-1/2 ( $\sigma, \sigma' = (1/2, 1/2)$ ). In Fig.7(a) we observe that without dimerization  $\gamma = 0$ , the spin-1/2-spin-1/2 correlation has a slower exponential fall-off than the spin-1-spin-1 case which means that the quantum fluctuations for spin-1/2 are stronger than the spin-1 case. Moreover, they both are positive which means that the spins are aligned parallel in each sublattice (ferro-magnetically). In Fig.7(b) we make a check by comparing with the one-dimensional case. This is achieved by using the “snake mechanism” [13]: we set  $\gamma = 1$  and  $J' = 2$  in eq. (1) for the SBA configuration. Under these conditions, we are dealing with an ordinary ferrimagnetic chain with alternating spins of magnitude 1/2 and 1 without dimerization and with effective coupling constant  $J_{eff} = 2$ . Thus, as we are plotting the connected correlation function

$$\langle S_0^z S_n^z \rangle - \langle S_0^z \rangle \langle S_n^z \rangle \quad (14)$$

then the case spin 1-1 has opposite sign and happens only in one-dimensional limit ( $J' = 2, \gamma = 1, SBA$ ). It is due to strong quantum fluctuations in the one-dimensional case. This is in full agreement with results obtained earlier in [3] (see Fig. 5(a) and (b) of this reference.) We have reproduced their results in a particular case of our study. Moreover, we have extended this numerical analysis for real 2-leg mixed spin ladders as explained in the other figures.

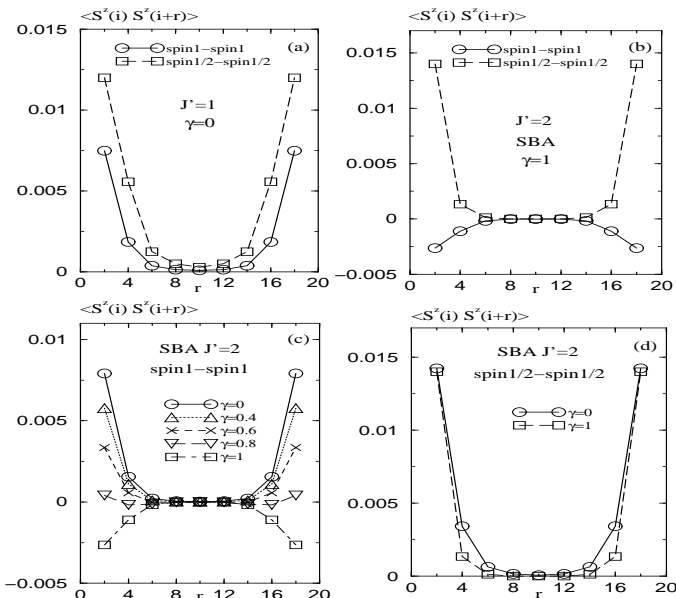


FIG. 7. Correlation functions for both spin (1/2, 1/2) and spin (1, 1) (Lanczos): (a) without dimerization; (b)-(d) with dimerization (SBA).

In order to see what is the effect of the interchain coupling  $J'$  on the correlation length  $\xi$  in the 2-leg ladder as compared with the pure one-dimensional case, we plot in Fig.7(d) the spin-1/2-spin-1/2 case for  $\gamma = 0$  and  $\gamma = 1$  at  $J' = 2$  and we observe that in the ladder ( $\gamma = 0$ ) there is a slower decay than in the chain ( $\gamma = 1$ ). This signals that the correlation length is bigger in the ferrimagnetic ladder than in the corresponding chain:  $\xi_{ladder} > \xi_{chain}$ . Likewise, in Fig. 7(c) we have made a similar analysis to see the effect of the dimerization in the staggered configurations (SBA). We observe that in the ladder  $\gamma \neq 1$  the correlation length  $\xi$  decreases as the dimerization gets stronger. Also, the correlations remain ferromagnetic in this spin-1 sub-lattice.

#### IV. NUMERICAL PHASE DIAGRAM

With the numerical tools provided by the Lanczos method we can also make an analysis of the phase diagram exhibited by the 2-leg mixed spin ladders in the space of couplings of the dimerization  $\gamma$  and the interchain coupling constant  $J'/J$ . We have performed this analysis for both antiferromagnetic couplings  $J' > 0$  and ferromagnetic couplings  $J' < 0$  (in units of  $J = 1$ ). Moreover, we have studied both dimerization patterns, CBA and SBA, considered throughout this work.

In order to set up this phase diagram we determine numerically the existence or lack of an energy gap in the lowest lying spectrum, as we have done in previous sections. For antiferromagnetic  $J'$  we find gapless ferrimagnetic order for both CBA and SBA configurations. This ferrimagnetic order is supported by a non-zero value of magnetization. This is in agreement with the approximate QRG analysis in [11], and thus we do not explicitly plot this diagram. The most interesting characteristics are found in the ferromagnetic  $J'$  region. In this case, we find that the GS is a spin singlet while the lowest excitation is a spin triplet. For the SBA dimerization pattern we always find a gapless behaviour for any value of the dimerization parameter  $\gamma$ . Since the ground state is a singlet the magnetization is zero for all  $J' < 0$  region. Thus we conclude that the phase boundary between the two gapless phases ( $J' < 0$  and  $J' > 0$ ) is at  $J' = 0$  where a first-order phase transition occurs. If we consider the magnetization as the order parameter then it is discontinuous at  $J' = 0$  (1-st order transition). The  $J' = 0$  transition line modifies the location of phase boundary obtained by QRG in the previous study (see Fig.3 in Ref. [11]).

However, the situation turns richer for the CBA dimerization and this is the case that we plot in Fig.8.

To obtain this numerical phase diagram we have split the range  $\gamma \in [0, 1]$  into 0.1 steps and the range  $J' \in [-2, 0]$  into 0.2 steps. Thus, we end up with a  $10 \times 10$  grid of numerical points. For each point in this grid, we have computed the lowest energy state in the sectors of total spin component  $S^z = 0, 1$ . This is done for a series of lattice sizes, namely,  $N = 2 \times L$  with  $L = 4, 6, 8, 10$ . With this data we extrapolate the value of the energy gap for infinite lattices and draw a symbols  $X$  if the gap is non-vanishing and a symbol  $O$  otherwise. These extensive Lanczos analysis is presented in Fig.8.

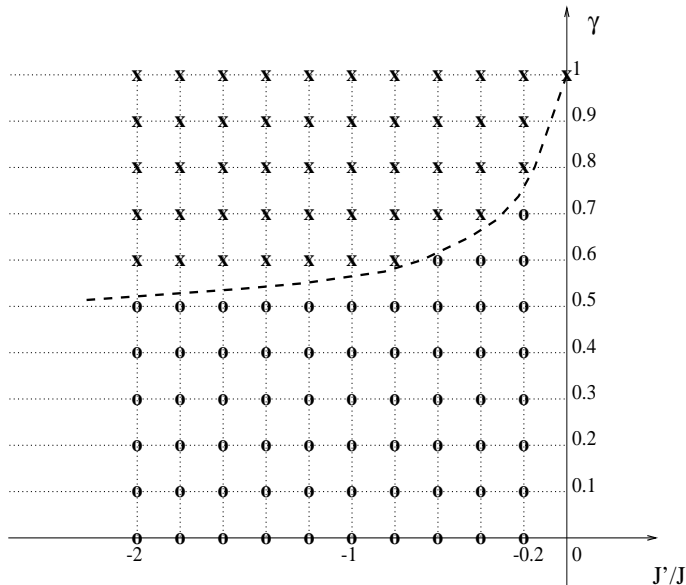


FIG. 8. Phase diagram of a 2-leg mixed spin ladder with CBA dimerization in the space of couplings  $\gamma$  v.s.  $J'/J$  ( $J' < 0$ ). A cross  $X$  symbol denotes a finite gap while an  $O$  symbol denotes a zero gap. The dashed line is an estimate for the phase boundary between the gapless and gapful phases.

Here we find two phases depending on whether we are in a strong or weak dimerization regime, assuming also that the interchain coupling  $J'$  is not negligible. We clearly detect a gapful phase in the upper part of the diagram and a gapless phase in the lower part. From our numerical data we also estimate the phase separating line plotted as a dashed line in Fig.8 and we observe that it approaches a horizontal asymptote as the interchain coupling becomes very large. As it has been mentioned before the whole  $J' < 0$  region has zero magnetization due to the spin of ground state which is  $S = 0$ . So the phase boundary between the two gapless phases ( $J' < 0$  and  $J' > 0$ ) is at  $J' = 0$  accompanying a first-order transition similar to SBA configuration.

## V. THE SPIN-PEIERLS INSTABILITY

We have also carried out a Lanczos study of the spin-Peierls (SP) instability. This phenomena has been realized in several materials and here we anticipate this possibility in the ferrimagnetic 2-leg ladders. This transition towards a dimerised GS ferrimagnetic ladder is determined by the competition between the lowering of the magnetic energy due to dimerization and the raising of the elastic energy due to phonons. According to standard terminology, the transition is called unconditional if the ground state is dimerised for arbitrary large value of the spin-phonon coupling (or small value of dimerization), and it is called conditional otherwise.

Using exact diagonalization techniques it has been possible to establish [16] that integer spin chains do not have a spin-Peierls transition while half-integer spin chains does exhibit this transition. This behaviour was predicted by Schulz [17] using bosonization techniques. However, other analytical studies had contradicted this conclusion [16]. Therefore, the study of the spin-Peierls transition provides us with an alternative view of the quantum differences between integer and half-integers spins, in addition to the more familiar gapped v.s. gapless behaviour.

Moreover, it is very interesting to study the SP transition for *quasi*-1D systems as a function of the interchain coupling  $J'$ . This is usually done within the so called chain mean-field theory which underestimates the effect of this coupling. Here we can treat its effect without any bias.

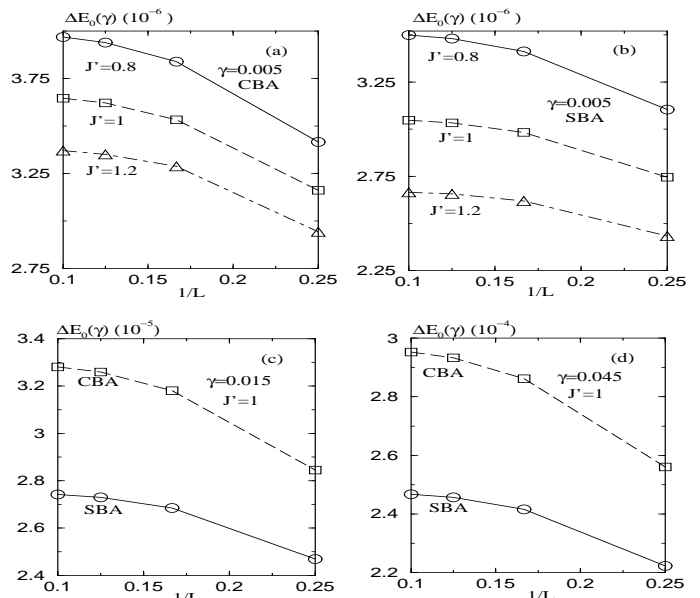


FIG. 9. Plot of the magnetic energy gain (Lanczos)  $\Delta E_0(\gamma)$  eq. (15) v.s.  $1/L$  for both CBA and SBA configurations (spin-Peierls analysis). (a) and (b) for different values of inter-chain coupling ( $J'$ ) and fixed value of  $\gamma = 0.005$ . Fixed value of  $J' = 1$  is presented in (c)  $\gamma = 0.015$  and (d)  $\gamma = 0.045$ .

The magnetic energy gain per bond  $\Delta E_0(\gamma)$  is computed as follows,

$$\Delta E_0(\gamma) = [E_L(0) - E_L(\gamma)]/L_b, \quad (15)$$

where  $L_b = 3L$  is the number of interacting bonds. It can be shown that studying the limit of (15) as  $L \rightarrow \infty$  for small  $\gamma$  reveals the conditional or unconditional character of the SP transition. Specifically, this feature is encoded in the concavity or convexity character, respectively, of the curve of (15) v.s.  $1/L$  [16]. Namely, for a finite system the condition for having an unconditional dimerised transition is that in the limit of small  $\gamma$ , the energy gain (15) must strictly increase as  $N$  increases. This means that the stabilization energy always overcomes the elastic energy. Otherwise, if the magnetic energy gain does not strictly increase with increasing the size, then the transition is conditional, i.e., it depends on the stiffness of the lattice. This characterization of the conditional v.s. unconditional character of the dimerization transition can be recasted in terms of the geometry of the curve for the energy magnetic gain (15) as a function of the size  $1/L$ : when the transition is unconditional the curvature of this function is oriented upwards with respect to the  $x$  axis and we call this a convex curve (see Fig.1(a)) in [16]); while in case of the conditional transition, the curvature is oriented downwards with respect to the horizontal axis and we call this a concave curve (see Fig.1(b) in [16].) In Figs. 9 we present our results. We observe that these curves are clearly concave for any values of the  $J'$  couplings that we have investigated. Moreover, this result holds true for both CBA and SBA configurations. Thus, we find that the SP transition is conditional for a set of values in  $J'$  ranging from 0 to 2.0. We have presented a reduced number of plots for the variation of  $J'$  in Fig.9 because for larger values the curves have a different scale and cannot be fitted into one plot.

We have checked this by taking three different value of  $\gamma$  (0.005, 0.015, 0.045). It has been also shown that the magnetic energy gain in CBA is bigger than in the SBA configuration which is in agreement with Fig.(5) where the CBA configuration is more stable than the SBA one against small perturbations.

## VI. CONCLUSIONS

This paper represents the first extensive numerical study using the Lanczos method of quantum ferrimagnetism in quasi-one dimensional models with a ladder structure. Previous numerical works have dwell upon truly one dimensional spin chains with alternating spins of magnitude  $(S_1, S_2) = (1, 1/2)$ .

We have presented our results regarding ground state properties of a 2-leg ladder with two patterns of dimerization: Columnar (CBA) and Staggered(SBA). Likewise,

we have seen how the GS properties evolve upon variation of the interchain coupling constant  $J'$  of the ladder.

Among the properties we have computed we mention the ground state energy, Antiferromagnetic gap, gapless behaviour of the Ferromagnetic excitations as we extrapolate our results to the thermodynamic limit, GS correlation functions and so on and so forth. These results have been contrasted with an approximate Spin Wave Theory analysis in the linear approximation and found a qualitative good agreement in some properties like the ground state energy, but not for the gaps. Moreover, we have performed a numerical analysis of when a spin-Peierls transition can occur and we have reported that this transition is conditional.

We have completed our Lanczos study of 2-leg mixed spin ladders with the inclusion of a numerical phase diagram which allows us to clarify the different gapless or gapful phases in the space of couplings of the model.

We believe that these results are of interest for researchers in the area of quantum spin systems that may want to know how the ferrimagnetism of a one-dimensional spin chain evolves when an extra chain is introduced and treated on equal footing.

**Acknowledgements** We acknowledge discussions with M. Abolfath, H. Hamidian, I. Peschel and G. Sierra. We would thank the Centro de Supercomputación Complutense for the allocation of CPU time in the SG-Origin 2000 Parallel Computer and also Max-Planck-Institut für Physik komplexer Systeme for computer time. M.A.M.-D. was supported by the DGES spanish grant PB97-1190.

- 
- [1] A. K. Kolezhuk, H.-J. Mikeska, and S. Yamamoto, Phys. Rev. **B55**, R3336 (1997).
  - [2] S. Brehmer, H.-J. Mikeska and S. Yamamoto, J. Phys. Cond. Matt. **9**, 3921 (1997);
  - [3] S. K. Pati, S. Ramasesha, and D. Sen, Phys. Rev. B **55**, 8894 (1997). J. Phys. Cond. Matt. **9**, 8707 (1997);
  - [4] S. Yamamoto, S. Brehmer and H.-J. Mikeska Phys. Rev. **B57**, 13610 (1998); S. Yamamoto and T. Fukui, Phys. Rev. **B57**, R14008 (1998); S. Yamamoto, T. Fukui, K. Maisinger and U. Schollwock, J. Phys. Cond. Matt. **10**, 11033 (1998).
  - [5] F. D. M. Haldane, Phys. Rev. Lett. **50**, 1153 (1983); Phys. Lett. **A93**, 464 (1983).
  - [6] M. Abolfath, H. Hamidian and A. Langari, cond-mat/9901063.
  - [7] Hagiwara et al., J. Phys. Soc. Jpn. **67**, 2209 (1998).
  - [8] Verdager et al. Phys. Rev. **B29**, 5144 (1984); Pei et al., Inorg. Chem. **27**, 47 (1988).
  - [9] E. Dagotto and T. M. Rice, Science **271**, 618 (1996).
  - [10] E. Dagotto, Rev. Mod. Phys. **66**, 763 (1994).
  - [11] A. Langari, M. Abolfath and M.A. Martin-Delgado, Phys. Rev. **B61**, 343 (2000).
  - [12] O. Kahn, Y. Pei, M. Verdager, J.P. Renard and J. Sletten, J. Am. Chem. Soc. **110**, 782 (1988).
  - [13] M. A. Martin-Delgado, R. Shankar and G. Sierra, Phys. Rev. Lett. **77**, 3443 (1996).



- [14] M. A. Martin-Delgado, J. Dukelsky and G. Sierra, Phys. Lett. **A 250**, 431 (1998).
- [15] E. Lieb and D. Mattis, J. Math. Phys. **3**, 749 (1962).
- [16] D. Guo, T. Kennedy and S. Mazumdar, Phys. Rev. **B41**, R9592 (1990).
- [17] H.J. Schulz, Phys. Rev. **B34**, 6372 (1986).